Nonlinear Dyn (2011) 66:509–521
DOI 10.1007/s11071-010-9929-6

ORIGINAL PAPER

A nonlinear visco-elastoplastic impact model and the coefficient of restitution

Ahmet S. Yigit · Andreas P. Christoforou · Majed A. Majeed

Received: 27 March 2010 / Accepted: 26 December 2010 / Published online: 18 January 2011

Abstract A visco-elastoplastic model for the impact between a compact body and a composite target is presented. The model is a combination of a nonlinear contact law that includes energy loss due to plastic deformation and a viscous element that accounts for energy losses due to wave propagation and/or damping. The governing nonlinear equations are solved numerically to obtain the response. A piecewise linear version of the model is also presented, which facilitates analytical solution. The model predictions are compared to those of the well-known and commonly used Hunt–Crossley model. The effects of the various impact parameters, such as impactor mass, velocity, plasticity, and damping, on the impact response and coefficient of restitution are investigated. The model appears to be suitable for a wide range of impact situations, with parameters that are well defined and easily calculated or measured. Furthermore, the resulting coefficient of restitution is shown to be a function of impact velocity and damping, as confirmed by published experimental data.

Keywords Impact · Nonlinear · Visco-elastoplastic contact · Coefficient of restitution

A.S. Yigit (✉) · A.P. Christoforou · M.A. Majeed
Department of Mechanical Engineering, Kuwait University, P.O. Box 5969, Safat 13060, Kuwait
e-mail: ahmet.yigit@ku.edu.kw

1 Introduction

Despite the presence of an extensive literature in impact dynamics, the choice of an adequate model for a given problem is still an important issue to be addressed. Even when a model appears to be adequate for a given situation, often determining the model parameters is not straightforward. Traditionally, impacts between relatively rigid compact bodies have been treated by utilizing the impulse-momentum principle with the coefficient of restitution to account for energy lost during impact [1–4]. Though quite simple, this approach suffers from several problems. First, in the presence of friction, the method can lead to inconsistent results [5]. Another problem is that when one or both of the impacting bodies are part of a flexible multi-body system, the value of the coefficient of restitution to be used is difficult to determine. Furthermore, this method requires an effective contact algorithm and intermittent solutions before and after impact, and this may cause implementation problems [6, 7].

In order to address these difficulties, a number of continuous models have been proposed. Most of these models are based on contact laws in the form of force-indentation relationships. The Hertz contact law, developed for perfectly elastic contact between nonconforming compact bodies (e.g., spheres), was one of the first models used for hard impacts at very low velocities [1]. Clearly, this model is not adequate for most impacts in practice, as some energy is dissipated due to plastic deformation, wave propagation, and other

effects. Therefore, a number of contact models have been developed which include a damping element to account for energy dissipation during impact [8–11]. Linear damping models based on the Kelvin–Voigt solid were shown to be inconsistent since they result in nonzero impact forces at the beginning and at the end of contact due to nonzero approach and rebound velocities. Hunt and Crossley [12] proposed to use a nonlinear damping model to overcome this difficulty. However, this model is a result of an ad hoc fix and does not rely on any physical explanation. Moreover, the model parameters are difficult to determine using the given material properties and geometric conditions and often are "tuned" based on experimental results [13]. Also, the additional nonlinearity introduced by the model unnecessarily complicates the solution method. Despite these difficulties, the Hunt–Crossley model gained popularity in recent years and has been used in a number of studies [14, 15].

As an alternative to stiffness/damping models, an elastoplastic contact law was proposed to account for energy losses due to local plastic deformation during impact [11, 16, 17]. The model parameters can be determined easily from geometric conditions and material properties, and it has been used successfully in impact situations involving compact bodies. Using this model, the coefficient of restitution was shown to be a function of impact velocity, which is consistent with the experimental evidence [11, 18, 19]. One drawback of this model is the fact that it does not account for energy loss due to wave propagation. In a real situation, the disturbance generated at the contact point travels through the body as elastic stress waves of finite speeds. These waves produce vibrations, and part of the impact energy is converted to vibration. If the impacting bodies are of similar size, the elastic waves can travel across the bodies many times before the impact event ends and are therefore not lost. However, if one of the bodies is relatively large, the waves in the larger body do not have sufficient time to be reflected from any boundary and, in essence, remain "trapped" in the body [11, 20]. When one of the impacting bodies is a slender structural element such as a beam or plate, a significant amount of energy is transferred to the structure in the form of vibrations. The elastoplastic contact law can still be used in this case provided that the global deformation of the structure is included in the model along with the local contact deformation (i.e., the larger body is modeled as a flexible element) [21]. In some cases, however, it is convenient to treat the bodies as "rigid." In this case, the amount of energy transferred to the "flexible" element should be considered for an accurate representation of the impact event. In order to do this, the energy loss due to wave propagation should be included along with the energy loss due to local plastic deformation or damage. The impact of a small mass on an "infinite" structure can be a good model for isolating the effect of wave propagation. In this case, the waves do not have sufficient time to reflect back from the boundaries, and there is no significant structural deformation during impact. Therefore, in the absence of local plastic deformation, the only energy loss is due to wave propagation.

The impact of a compact body (e.g., a sphere) with an "infinite structure" (e.g., a large plate) was studied both analytically and experimentally [22, 23]. It was shown that the impact force is proportional to the velocity at the impact point, and a viscoelastic model similar to a Maxwell model was shown to govern the local contact behavior. In this case, the energy lost in "damping" represents the energy lost to the structure, and the damping coefficient can be determined from structural and material properties.

From the foregoing discussion, it can be concluded that if the elastic element in the Maxwell model is replaced by an elastoplastic element, the effects of both local plastic deformation and wave propagation can be accounted for. Ismail and Stronge [24] proposed a modified Maxwell model for impacts of viscoplastic bodies. They replaced the linear spring of the Maxwell model with a bilinear stiffness element to account for energy losses due to plastic deformation in the contact zone. Their model uses an ad hoc plastic loss factor in addition to the damping coefficient as model parameters. Though not explicitly stated, these model parameters were implied to be material properties. They concluded that their viscoplastic model, like the linear viscoelastic Maxwell model, results in a coefficient of restitution that is independent of impact velocity, which clearly contradicts the experimental evidence that the coefficient of restitution is indeed a function of impact velocity. The main objective of this work is to present a nonlinear visco-elastoplastic impact model where both the elastic-plastic stiffness and the damping behavior are derived based on well-defined elastoplastic contact and impact of a compact body with an infinite structure. Unlike some models that require tuning of parameters to match a certain

impact response [13], the parameters of the proposed model are well defined and can easily be calculated or measured a priori. The model can be used for a wide range of impact situations involving rigid body dynamics, wave propagation, viscoelasticity, and plasticity. Furthermore, the model predicts a consistent coefficient of restitution, which is a function of impact velocity and damping as confirmed by published experimental data.

2 Impact model

In the case of impact between a spherical object having an initial velocity of v_0 and a visco-elastoplastic half-space, or an infinite structure (see Fig. 1), the motion of the impactor is described by

$$m\ddot{\alpha} = -F, \tag{1}$$

$$c\dot{y} = F, \tag{2}$$

where m is the mass of the impactor, α is the total displacement of the impactor, c is the damping coefficient, which represents either the viscous dissipation in the material, or the effect of energy lost to the waves which do not have sufficient time to be reflected back from the boundaries, y is the dashpot displacement, and F is the impact force to be obtained from a contact law given as

$$F = \begin{cases} f(z), & \text{if } F > 0, \\ 0, & \text{if } F \le 0, \end{cases} \tag{3}$$

where z is the relative deformation in the spring defined as

$$z = \alpha - y. \tag{4}$$

The initial conditions are described as $\alpha(0) = y(0) = z(0) = \dot{y}(0) = 0$ and $\dot{\alpha}(0) = \dot{z}(0) = v_0$.

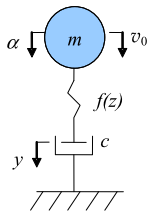

Fig. 1 Sketch of the model for nonlinear visco-elastoplastic impact

The value of the damping coefficient c can be calculated as in [20, 23, 25]: For the energy lost to axial waves (in the case of a relatively long slender element), $c = \rho A\sqrt{E/\rho}$, where ρ and E are the material density and Young's modulus, respectively, and A is the cross-sectional area of an effective infinite bar. For the energy lost to transverse waves (in the case of a relatively large thin element such as a plate), $c = 8\sqrt{\rho h D^*}$, where h is the thickness and D^* is the effective bending stiffness of the structure. In a general case of a small compact body impacting a large structure, both axial and transverse waves are generated. In this case, these two damping elements can be thought of as combined in series. As is clear from Fig. 1 and the foregoing equations, for the purpose of presentation of the impact model, it is assumed that all deformation occurs in a relatively small contact region, and the remaining parts of the bodies are assumed to be rigid otherwise.

Hertz contact law In cases where impacts are elastic in nature (i.e., no plastic deformation or damage), the classical Hertz contact theory [1, 11] may be used to obtain the impact force. The relationship between the contact force and local deformation for an elastic sphere and an elastic half-space is given as

$$F = K_h z^{3/2}, \tag{5}$$

where K_h is the Hertzian contact stiffness given as

$$K_h = \frac{4}{3}\sqrt{R}E^*. \tag{6}$$

In the above equation, R is the radius of the impactor, and E^* is the effective contact modulus given as

$$\frac{1}{E^*} = \frac{1-\nu_1^2}{E_1} + \frac{1-\nu_2^2}{E_2}, \tag{7}$$

where ν_i and E_i are the Poisson ratios and elastic moduli of the two contacting bodies, respectively. In the case of a composite laminate, a transversely isotropic material is assumed for the half-space [16, 26], and the corresponding elastic modulus is taken to be that of the transverse modulus of a ply, i.e., $E_2 = E_{22}$.

It is important to note here that when the Hertzian elastic contact law is used alone, the coefficient of restitution, which is a measure of the severity of impact, is always equal to unity. This is correct as long

as the deformation is elastic and there is no plastic deformation or damage. It is well known, however, that there is energy loss due to local damage and plastic deformation even for relatively low impact velocities [1, 11]. Therefore, the Hertzian contact law has been used as part of more complicated elastoplastic contact laws that account for damage effects due to plastic or permanent deformation. Such a contact law and its linearized version are explained in detail in the following section.

Elastoplastic contact law Experimental evidence suggests that during impact between metallic bodies, even at very low impact velocities, the contact stresses are high enough to cause material yielding, and thus plastic deformation [11]. A similar behavior was observed in the case of composite laminates where lateral contact loads cause permanent indentation [26, 27]. In the case of composite materials, the term "yielding" denotes a combination of different failure modes such as matrix and fiber damage.

In order to account for permanent deformation, an elastoplastic contact law [16] may be used to obtain the impact force. The contact law was obtained by combining the classical Hertzian contact theory [1] and the elastic-plastic indentation theory given in [11]. The contact consists of three phases, namely, elastic Hertzian loading, elastic-plastic loading where the contact is assumed to exceed a threshold value and it includes both elastic and plastic deformation, and elastic Hertzian unloading. The contact law is given as follows [16].

Phase I: *Hertzian elastic loading*

$$F = K_h z^{3/2}, \quad 0 \le z \le z_y. \tag{8}$$

Phase II: *Elastic-plastic loading*

$$F = K_y(z - z_y) + K_h z_y^{3/2}, \quad z_y \le z \le z_m. \tag{9}$$

Phase III: *Hertzian elastic unloading*

$$F = K_h\left(z^{3/2} - z_m^{3/2} + z_y^{3/2}\right) + K_y(z_m - z_y), \tag{10}$$

where z_y is the deformation where yielding or damage occurs and is given as

$$z_y = \frac{0.68 S_y^2 \pi^2 R}{E^{*2}} \tag{11}$$

and S_y is the yield strength for metals, and $S_y = 2S_u$ for composite laminates with S_u being their shear strength. K_y is the linear contact stiffness of the elastic-plastic loading phase, which is the slope of the force-deformation curve at z_y and is given as

$$K_y = 1.5 K_h \sqrt{z_y}. \tag{12}$$

Finally, z_m is the maximum spring deformation. Note that the transition from compression to restitution occurs at maximum impactor displacement, α_c, i.e., when the impactor velocity vanishes:

$$\dot{\alpha}(t_c) = 0. \tag{13}$$

It is important to note that, in the presence of damping, this transition occurs after the time of maximum impact force, and $z_m < \alpha_c$; in other words, the maximum impactor displacement is reached after the maximum impact force.

As mentioned earlier, the severity of impact can be assessed by the coefficient of restitution. There are three definitions: Newton (kinematic), Poisson (kinetic), and energetic [4]. Depending on the problem, these definitions result in different values for the coefficient of restitution. However, if friction is not present, which is the case considered here, all definitions give the same result [4]. Newton's definition for the coefficient of restitution is the easiest as it involves the ratio of the relative velocities of the impactor and the target after and before impact. It is simply given as

$$e = -\frac{\dot{\alpha}(t_f)}{\dot{\alpha}(0)} = -\frac{\dot{z}(t_f)}{v_0}. \tag{14}$$

In previous work it was shown that the elastoplastic contact law can be used effectively in the impact of compact bodies as well as flexible structures [16, 21]. Physically consistent results for the coefficient of restitution for the impact of spherical objects on thick composite laminates and for the impact response of flexible structures with local contact damage were obtained. Furthermore, a linearized contact law was used to obtain simple, yet informative, results for the nondimensional response of structures [21, 25]. The linear contact law, however, was elastic in nature, and the effect of permanent deformation was neglected. Therefore, a piecewise linear elastoplastic contact law is now proposed. The loading and unloading phases of the contact law are obtained by neglecting the initial elastic loading phase and by linearizing the elastic-plastic loading and elastic unloading phases of the nonlinear elastoplastic law given in (8)–(10). The two

phases of the linearized contact law are given as follows.

Phase I: *Loading*

$$F = K_y z, \quad 0 \le z \le z_m. \tag{15}$$

Phase II: *Unloading*

$$F = \frac{K_y}{\gamma^2}(z - z_f), \tag{16}$$

where z_f is the permanent spring deformation, which is obtained as

$$z_f = z_m\left(1 - \frac{K_y}{K_h\sqrt{z_m}}\right)^{2/3} \tag{17}$$

and γ is the plastic loss factor as defined in [24], which is obtained as

$$\gamma^2 = 1 - \frac{z_f}{z_m} = 1 - \left(1 - \frac{K_y}{K_h\sqrt{z_m}}\right)^{2/3}. \tag{18}$$

It is important to note here that the plastic loss factor γ is the coefficient of restitution when there is no damping or wave propagation effect. In such cases, the transition from compression to restitution occurs at maximum impact force and deformation, and $z_m = \alpha_c$. It is easy to show that the impact model, (1)–(4), without damping, along with the linearized contact law given by (15)–(17), predicts this transition as

$$z_m = \alpha_c = v_0\sqrt{\frac{m}{K_y}}. \tag{19}$$

Substituting (19) into (18) yields

$$\gamma^2 = 1 - \left[1 - \left(\frac{K_y}{K_h}\right)\left(\frac{K_y}{m v_0^2}\right)^{1/4}\right]^{2/3}. \tag{20}$$

For low velocities, there is no significant permanent deformation, and the coefficient of restitution is close to unity. For large velocities that cause significant permanent deformation, (20) can be simplified by using the binomial theorem, and the plastic loss factor, or in this case the coefficient of restitution, can be obtained as

$$\gamma^2 = \frac{2}{3}\left(\frac{K_y}{K_h}\right)\left(\frac{K_y}{m v_0^2}\right)^{1/4}. \tag{21}$$

Equation (21) clearly shows the $(v_0)^{-1/4}$ dependence of the coefficient of restitution as observed in experiments (see p. 363 in [11]). This analytical expression is only possible because of the appropriate linearization of the nonlinear elastoplastic contact law given before. As mentioned above, the contact stiffness during the loading phase, K_y, is taken as the slope of the elastic Hertzian loading curve at z_y. As is clear from (11), this value depends on the material properties and geometry of the impactor. The stiffness during the unloading phase is obtained by a secant linearization of the elastic unloading curve. Unlike the slope of the loading phase, the linear unloading stiffness also depends on the impact energy (21). Though intuitive, this result is significant in accounting for the effect of impact velocity on the coefficient of restitution, which was overlooked by some researchers [24].

When the nonlinear elastoplastic contact law given by (8)–(13) is used, no analytical solution exists, and the problem must be solved numerically. However, it is possible to obtain an analytical solution when the linearized elastoplastic contact law given by (15)–(19) is used. Analytical solutions are useful for validating computational results and for conducting parametric studies. These solutions are straightforward once the piecewise linear equations are obtained as follows.

Phase I: *Loading*. Substituting (15) into (1) and (2) and utilizing (4), the equations of motion can be combined into a single equation for the spring deformation:

$$\ddot{z} + 2\zeta\omega_0\dot{z} + \omega_0^2 z = 0, \tag{22}$$

where ω_0 is the undamped natural frequency, and ζ is the damping ratio given, respectively, as

$$\omega_0 = \sqrt{\frac{K_y}{m}}, \qquad \zeta = \frac{\sqrt{m K_y}}{2c}. \tag{23}$$

The initial conditions are the same as prescribed earlier; $z(0) = 0$ and $\dot{z}(0) = v_0$.

Phase II: *Unloading*. Following the same procedure used in the loading phase, but instead using the unloading equations of the contact law, (16)–(18), the equation of motion for the unloading phase is obtained as

$$\ddot{z} + 2\zeta_1\omega_1\dot{z} + \omega_1^2 z = \omega_1^2\left(1 - \gamma^2\right)z_m, \tag{24}$$

where

$$\omega_1 = \frac{\omega_0}{\gamma}, \qquad \zeta_1 = \frac{\zeta}{\gamma} \tag{25}$$

are the natural frequency and damping ratio for the unloading phase, respectively. The initial conditions are the spring deformation and velocity at maximum impact force, i.e., $z(t_m) = z_m$ and $\dot{z}(t_m) = 0$. Solutions to (22)–(25) are readily available. Once the analytical expressions for the spring deformation $z(t)$ are obtained, the impact force and the impactor displacement can easily be calculated.

Also, it is convenient to present some of the results in a normalized form. The time, indentation, and impact force are normalized as follows:

$$\tau = \omega_0 t, \qquad \bar{\alpha} = \frac{\alpha}{v_0/\omega_0}, \qquad \bar{F} = \frac{F}{m v_0 \omega_0}. \tag{26}$$

3 Simulation results and discussion

In the following, the simulation results of the impact of a 0.5 kg hemispherical steel impactor of radius $R = 10$ mm and a composite target are presented. The material properties of the two impacting bodies used in the simulations (unless otherwise stated) are given in Table 1. Figures 2–7 show the comparisons of nonlinear and linear solutions for the impact force history and the resulting hysteresis diagrams for a set of impactor velocity values. In these figures, the nonlinear solutions are obtained by numerically solving (1)–(4), with the impact force given by (8)–(10). The linear solutions are obtained by analytically solving (1)–(4) (or (22)–(24)), with the impact force given by (15)–(16). The parameters used in these cases along with a damping coefficient, $c = 11440$ Ns/m, result in a damping ratio of $\zeta = 0.1$. Also shown in these figures are the results from the well-known Hunt–Crossley model [12], for which the impact force is given as

$$F = K\alpha^{3/2}(1 + \mu\dot{\alpha}) \tag{27}$$

where K and μ are the model parameters that need to be chosen to obtain a desired impact response (e.g., experimental data) [28]. Here, these parameters are selected to yield the same maximum impact force and coefficient of restitution as predicted from the proposed impact model. The Hunt–Crossley model results are obtained by numerically solving (1) with the impact force given by (27).

At low speeds ($v_0 = 0.1$ m/s), the impact response is elastic and follows a Hertzian type of contact law. As can be seen in Figs. 2 and 3, the predictions by the nonlinear and Hunt–Crossley ($K = 9.28 \times 10^8$, $\mu = 4.4$) models are very close to each other. On the

Table 1 Material properties used in the simulations

Composite laminate (*target*)
$[0/90/0/90/0]_s$ T300/934 carbon-epoxy
$E_{11} = 120$ GPa, $E_{22} = 7.9$ GPa, $G_{12} = G_{23} = 5.5$ GPa,
$S_u = 101$ MPa
$\nu_{12} = \nu_{23} = 0.3$, $\rho = 1580$ kg/m^3
Steel (*impactor*)
$E = 207$ GPa, $\nu = 0.3$, $\rho = 7960$ kg/m^3

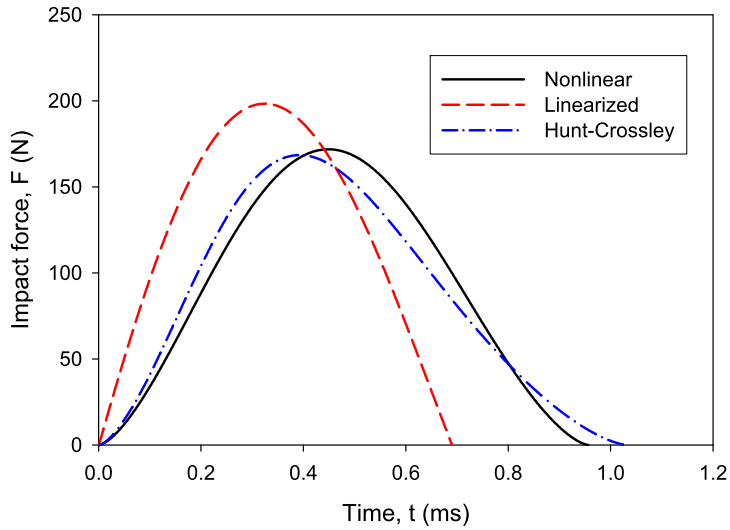

Fig. 2 Model predictions for the impact response with no plastic deformation, $v_0 = 0.1$ m/s

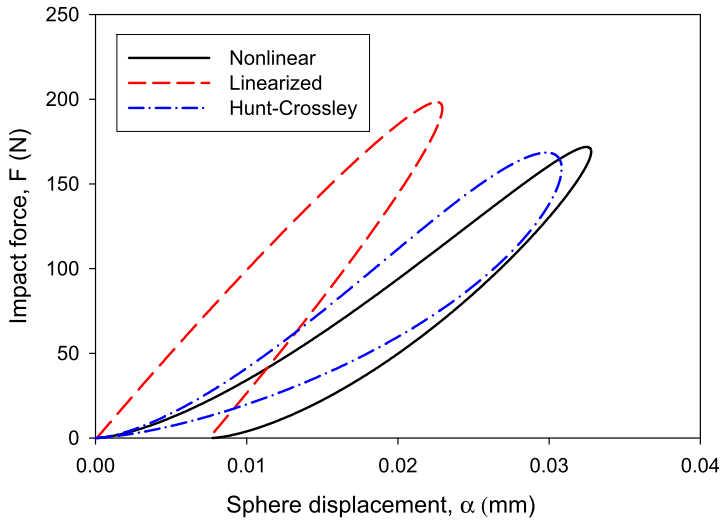

Fig. 3 Impact force-displacement relationships with no plastic deformation, $v_0 = 0.1$ m/s

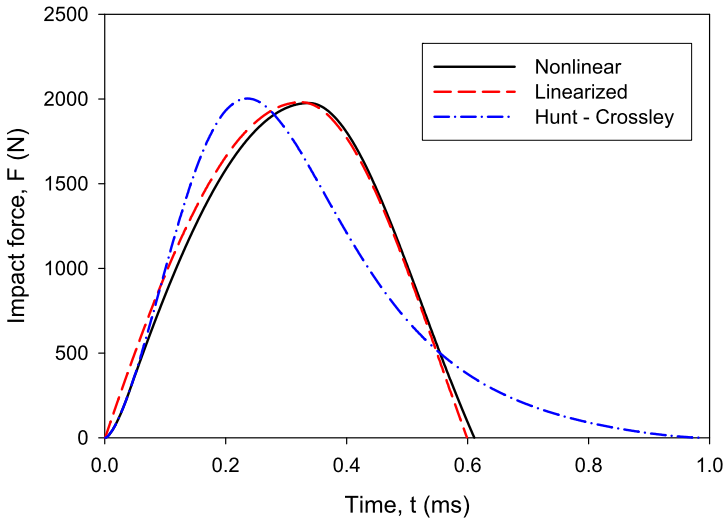

Fig. 4 Model predictions for the impact response with moderate plastic deformation, $v_0 = 1$ m/s

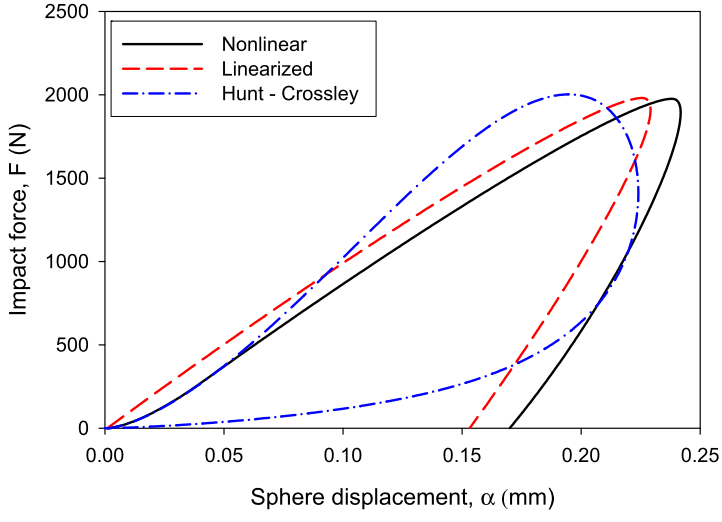

Fig. 5 Impact force-displacement relationships with moderate plastic deformation, $v_0 = 1$ m/s

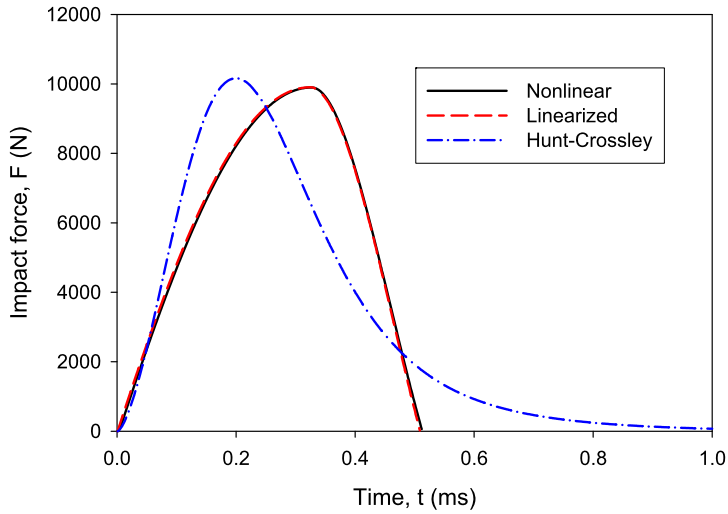

Fig. 6 Model predictions for the impact response with large plastic deformation, $v_0 = 5$ m/s

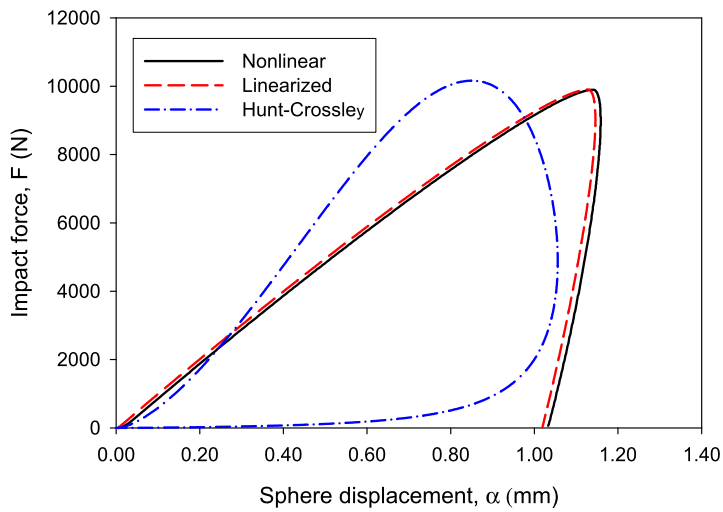

Fig. 7 Impact force-displacement relationships with large plastic deformation, $v_0 = 5$ m/s

other hand, using the linear contact law overestimates the impact force. It should be noted that the apparent permanent deformation shown in Fig. 3 is due to the limitation of the Maxwell-type viscoelastic model, which is valid only during contact. This type of viscoelastic model will predict permanent deformation at the dashpot, since there is no elastic element parallel to it. In a real case, when the load is removed (i.e., once impact is over), this deformation is eventually restored through the elastic compliance and inertia of the half-space, which are not included in the model. Certainly, the model can be improved by adding a spring parallel to the dashpot (similar to the standard solid model). However, this is not done since the effect is negligible for most impacts where there is significant energy loss due to plastic deformation.

At higher velocities, and once permanent deformation is present, the nonlinear and linear predictions are very close to each other, which can be clearly seen in Figs. 4–7. Figures 4 and 5 show the model predictions when the impactor velocity is 1 m/s that causes moderate plastic deformation. The Hunt–Crossley model parameters used in this case are $K = 4.2 \times 10^8$, $\mu = 1.608$. As can be seen, the linearized model provides an excellent approximation to that of the nonlinear model. As mentioned above, the parameters for the Hunt–Crossley model are chosen to yield the same maximum impact force and energy dissipation

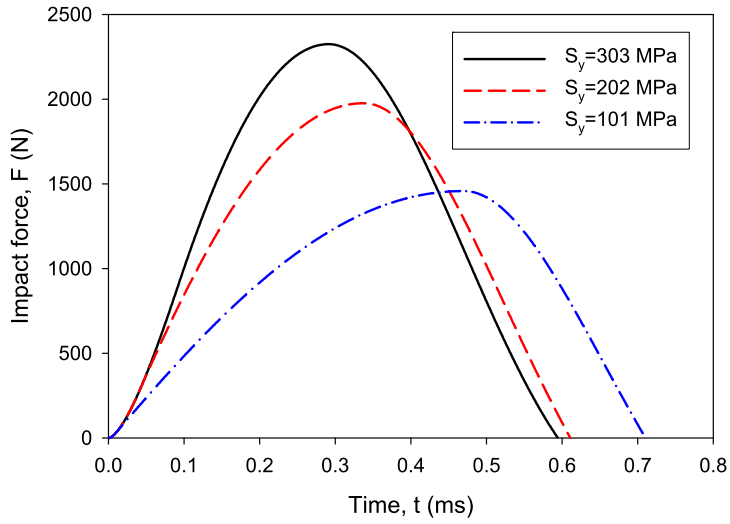

Fig. 8 Effect of plasticity on the impact response, $v_0 = 1$ m/s

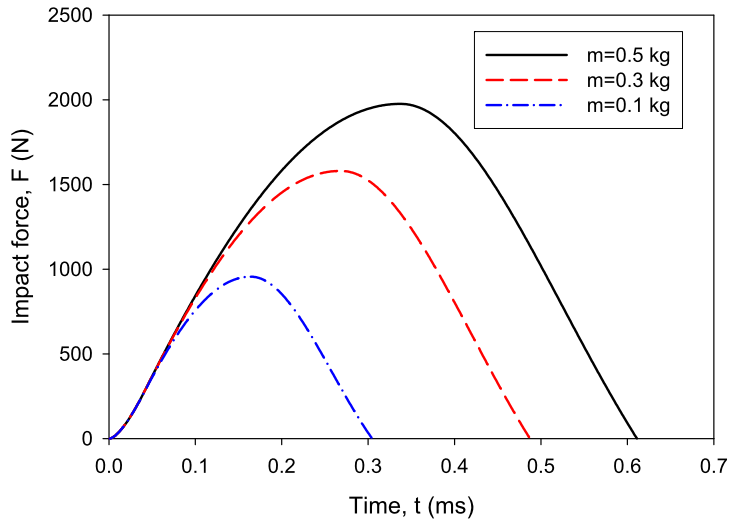

Fig. 9 Effect of impactor mass on the impact response, $v_0 = 1$ m/s

of nonlinear visco-elastoplastic model. As can be seen from Figs. 4 and 5, the resulting maximum forces, although not identical, are reasonably close to each other such that two model predictions can be compared. The Hunt–Crossley model overpredicts the impact duration to compensate for the permanent deformation which is not accounted for. Also, the maximum indentation is smaller with the Hunt–Crossley model as shown in Fig. 5, indicating that it has larger impedance than that of the visco-elastoplastic model. Figures 6 and 7 show the simulation results for an impact velocity of 5 m/s, which results in a large plastic deformation. There is an excellent agreement between the linearized and nonlinear model predictions. The Hunt–Crossley model behaves similarly as in the previous case.

Figure 8 shows the effect of plasticity on the impact response using the proposed nonlinear visco-elastoplastic impact model. As the yield strength decreases, the contact stiffness decreases, resulting in smaller impact forces and longer impact durations. The effect of impactor mass is shown in Fig. 9. As the impactor mass decreases, the maximum impact force decreases due to the decrease in impact energy. Also, the impact duration decreases with decreasing impactor mass.

In the rest of the simulations the normalized responses are chosen for easy and clear presentation,

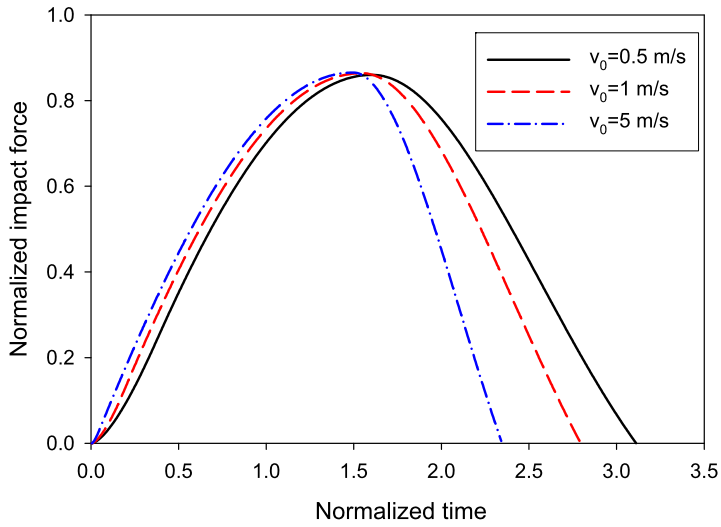

Fig. 10 Effect of velocity on the normalized impact response, $\zeta = 0.1$

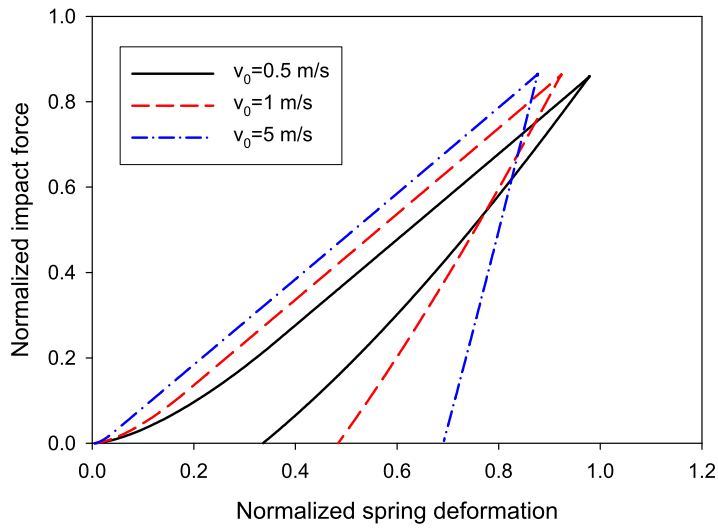

Fig. 11 Effect of velocity on the normalized force-deformation relationships, $\zeta = 0.1$

as they can be placed on the same figure even if the dimensional results are different by an order of magnitude. Since some low-velocity impacts are included, the numerical solutions to the nonlinear model are presented. Figures 10 and 11 show the effects of velocity on the normalized impact response when the damping ratio is constant. As it can be seen in Fig. 10, the impact duration decreases with increasing impact velocity due to the increase of plastic deformation, which is shown in Fig. 11. As predicted by the analytical results, when the impact velocity increases the plastic loss factor decreases (21), and the slope of the unloading phase of the contact law increases (16). The effect of nonlinearity (Hertzian) is visible in the initial stages of loading and it gets smaller as the velocity increases. Figures 12 and 13 show the effects of the damping ratio on the normalized impact response when the impact velocity is constant. As expected, a higher damping ratio decreases the maximum impact force and increases the impact duration. Figure 13 indicates that the plastic loss factor is the same, as seen by the same slope in the unloading phase. However, the plastic deformation in the spring decreases with increasing damping ratio due to decreasing maximum impact force.

The effects of impact velocity and damping ratio on the coefficient of restitution are shown in Fig. 14. For a given impact velocity, increasing the damping

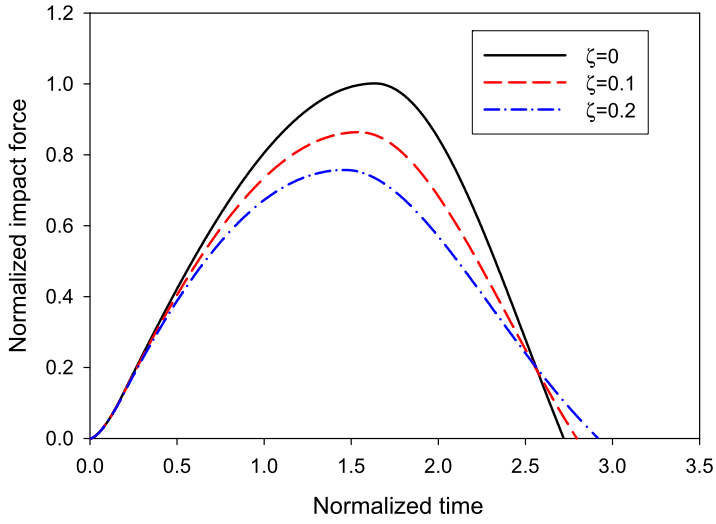

Fig. 12 Effect of damping ratio on the normalized impact response, $v_0 = 1$ m/s

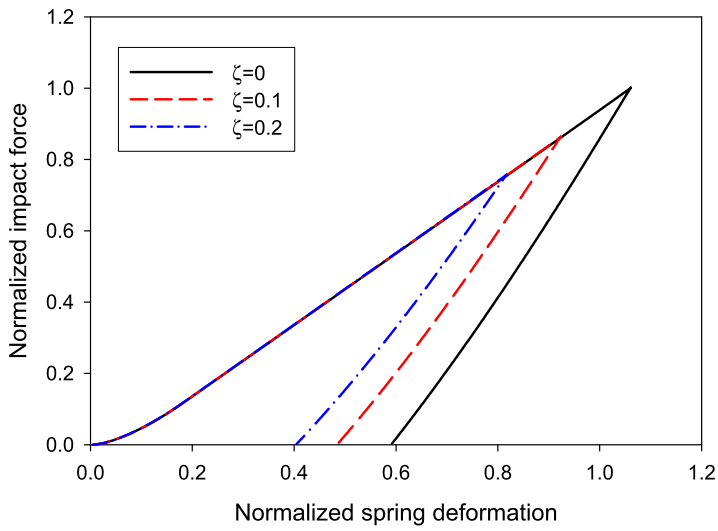

Fig. 13 Effect of damping ratio on the normalized force-deformation relationships, $v_0 = 1$ m/s

ratio results in lower values of the coefficient of restitution. The coefficient of restitution decreases as the impact velocity increases, which is consistent with experimental data. This result is in contrast to that of the linear Maxwell viscoelastic and viscoplastic models, where the coefficient of restitution is independent of impact velocity [24].

4 Conclusions

A nonlinear impact model that incorporates energy losses due to plastic deformation, viscoelastic material behavior, and wave propagation has been developed and used to study impacts of a compact body and a composite target. The governing equations of motion have been linearized, enabling analytical solutions with excellent agreement with the numerical solutions at moderate to high impact velocities. The model predictions have been compared to those of the well-known Hunt–Crossley model. The analytical solutions facilitated by the linearization are helpful in identifying the effects of the various impact parameters, such as impactor mass and velocity, and material properties, such as plasticity and damping, on the impact response and coefficient of restitution. It has been shown that the coefficient of restitution is a function

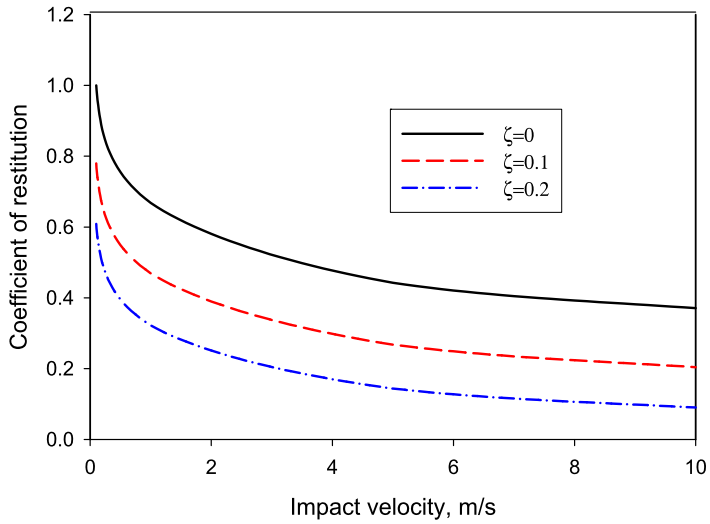

Fig. 14 Variation of the coefficient of restitution with damping ratio and impact velocity

of both the damping ratio and the impact velocity. It is expected that the proposed model can be useful in parametric and experimental studies and in validating computational (FE) models.

Acknowledgement This work was supported by Kuwait University Research Grant No. [EM-03/07].

References

1. Goldsmith, W.: Impact. Edward Arnold, SevenOaks (1960)
2. Khulief, Y.A., Shabana, S.A.: Impact response of multibody systems with consistent and lumped masses. J. Sound Vib. **104**(2), 187–207 (1986)
3. Yigit, A.S., Ulsoy, A.G., Scott, R.A.: Dynamics of a radially rotating beam with impact, Part 1: Theoretical and computational model. J. Vib. Acoust. **112**, 65–70 (1990)
4. Stronge, W.J.: Impact Mechanics. Cambridge University Press, Cambridge (2000)
5. Wang, Yu., Mason, M.T.: Two dimensional rigid-body collisions with friction. J. Appl. Mech. **59**, 635–642 (1992)
6. Yigit, A.S., Christoforou, A.P.: The efficacy of the momentum balance method in transverse impact problems. J. Vib. Acoust. **120**, 47–53 (1998)
7. Escalona, J.L., Mayo, J.M., Dominguez, J.: Critical study of the use of the generalized impulse-momentum balance equations in flexible multibody systems. J. Sound Vib. **217**(3), 523–545 (1998)
8. Dubowsky, S., Freudenstein, F.: Dynamic analysis of mechanical systems—Part 1: Formation of dynamical model. J. Eng. Ind. **93**, 305–309 (1971)
9. Khulief, Y.A., Shabana, A.A.: A continuous force model for the impact analysis of flexible multibody systems. Mech. Mach. Theory **22**, 213–224 (1987)
10. Lankarani, H.M., Nikravesh, P.E.: Continuous contact force models for impact analysis in multi-body systems. Nonlinear Dyn. **5**, 193–207 (1994)
11. Johnson, K.L.: Contact Mechanics. Cambridge University Press, Cambridge (1985)
12. Hunt, K.H., Crossley, F.R.E.: Coefficient of restitution interpreted as damping in vibroimpact. J. Appl. Mech. **42**, 440–445 (1975)
13. Gilardi, G., Sharf, I.: Literature survey of contact dynamics modeling. Mech. Mach. Theory **37**, 1213–1239 (2002)
14. Anderson, R.W.G., Long, A.D., Serre, T.: Phenomenological continuous-impact modeling for multibody simulations of pedestrian-vehicle contact interactions based on experimental data. Nonlinear Dyn. **58**, 199–208 (2009)
15. Zhang, Y.N., Sharf, I.: Validation of nonlinear viscoelastic contact force models for low speed impact. J. Appl. Mech. **76**(5), 051002 (2009)
16. Yigit, A.S., Christoforou, A.P.: On the impact of a spherical indenter and an elastic-plastic transversely isotropic half-space. Compos. Eng. **4**(11), 1143–1152 (1994)
17. Wu, C., Li, L., Thornton, C.: Energy dissipation during normal impact of elastic and elastic-plastic spheres. Int. J. Impact Eng. **32**, 593–604 (2005)
18. Zhang, X., Vu-Quoc, L.: Modeling the dependence of the coefficient of restitution on the impact velocity in elasto-plastic collisions. Int. J. Impact Eng. **27**, 317–341 (2002)
19. Wu, C., Li, L., Thornton, C.: Rebound behavior of spheres for plastic impacts. Int. J. Impact Eng. **28**, 929–946 (2003)
20. Zener, C., Feshbach, H.: A method of calculating energy losses during impact. J. Appl. Mech. **61**, A67–A70 (1939)
21. Christoforou, A.P., Yigit, A.S.: Effect of flexibility on low velocity impact response. J. Sound Vib. **217**, 563–578 (1998)
22. Doyle, J.F.: Experimentally determining the contact force during the transverse impact of an orthotropic plate. J. Sound Vib. **118**(3), 441–448 (1987)
23. Doyle, J.F.: Wave Propagation in Structures: An FFT-Based Spectral Analysis Methodology. Springer, New York (1989)
24. Ismail, K.A., Stronge, W.J.: Impact of viscoplastic bodies: dissipation and restitution. J. Appl. Mech. **75**(6), 061011 (2008)

25. Christoforou, A.P., Yigit, A.S.: Scaling of low-velocity impact response in composite structures. Compos. Struct. **91**, 358–365 (2009)
26. Tan, T.M., Sun, C.T.: Use of statical indentation laws in the impact analysis of laminated composite plates. J. Appl. Mech. **52**, 6–12 (1985)
27. Swanson, S.R., Rezaee, H.G.: Strength loss in composites from lateral contact loads. Compos. Sci. Technol. **38**, 43–54 (1990)
28. Arz, J.P., Laville, F.: Experimental characterization of small thickness elastomeric layers submitted to impact loading. J. Sound Vib. **326**, 302–313 (2009)